Solar Energy 311 (2026) 114529

Contents lists available at ScienceDirect

Solar Energy

journal homepage: www.elsevier.com/locate/solener

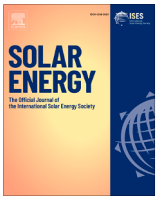

Evaluation of the panel temperature modeling parameters for bifacial photovoltaics with open-rack and vertical installations

Julianna Varjopuro [a,*], Aleksi Kamppinen [a], Aapo Poskela [a], Anders V. Lindfors [b], Shuo Wang [c], Samuli Ranta [c], Kati Miettunen [a]

[a] Department of Mechanical and Materials Engineering, University of Turku, Vesilinnantie 5, Turku, 20500, Finland
[b] Finnish Meteorological Institute, Erik Palmenin aukio 1, Helsinki, 00560, Finland
[c] Turku University of Applied Sciences, Joukahaisenkatu 7, Turku, 20520, Finland

HIGHLIGHTS

- Applicability of photovoltaic temperature models to bifacial panels has been validated.
- Model parameters and panel temperatures can be reliably predicted using simulations.
- Panel-specific model parameters improve the temperature estimations.

ARTICLE INFO

Keywords:
Thermal modeling
Bifacial photovoltaics
Vertical installation
Panel temperature
Temperature prediction

ABSTRACT

Bifacial photovoltaics have rapidly gained significant market share; however, their thermal modeling is lagging behind. Reliable thermal modeling contributes to more robust predictions of the temperature-dependent output power, which emphasizes the need for accurate thermal models for emerging photovoltaic technologies. This study addresses the literature gap related to the validation of thermal models for bifacial photovoltaic (PV) systems. Key novelties include extending the investigation of bifacial PV temperature models to vertical installations and providing insights into their accuracy in challenging Nordic conditions. The applicability of common PV temperature models to bifacial panels was evaluated using experimental data collected from two bifacial systems with vertical and open-rack mounting. Temperature model parameters of Sandia, Faiman and PVsyst models for bifacial panels were extracted from both experimental and computationally simulated temperature data to investigate the use of computational methods in predicting model parameters and panel temperature. The good matching of experimental and simulated parameters with different installation geometries suggests that simulation is a powerful method to identify new parameters for solar devices with different material combinations and cell technologies. Further, one of the key questions was whether standard temperature model parameters—originally developed for monofacial panels—are suitable for bifacial panels. The results revealed that replacing the standard model parameters with bifacial-specific ones enhanced the accuracy of temperature estimation in all cases studied, e.g., for open-rack mounted bifacial panel 0.2 – 1.2 °C depending on the temperature model. Overall, the findings of the study improve the prediction of power output of bifacial panels in different installations.

1. Introduction

Global installed photovoltaic (PV) capacity is expected to increase significantly in the coming decades [1,2]. Industry and national energy systems should prepare for the change to minimize potential challenges, for instance, dramatic electricity price fluctuations and collapses in solar power capture rates [3]. Applications of bifacial photovoltaic (BPV) cells are accelerating the growth of solar power production due to their ability to absorb sunlight from both the front and rear surfaces [4,5]. The challenge is that the rapid increase in PV capacity will reduce the price of electricity and, thus, the profits resulting from the PV system at solar noon [3,6]. To avoid this so-called self-cannibalism, new ways to improve grid stability are actively explored. For instance, east-west oriented vertically installed bifacial photovoltaic (VBPV) panels shift

* Corresponding author.
Email address: julianna.varjopuro@utu.fi (J. Varjopuro).

https://doi.org/10.1016/j.solener.2026.114529
Received 23 January 2026; Received in revised form 4 March 2026; Accepted 13 March 2026
Available online 21 March 2026

the production peak from noon to morning and evening, which aligns well with the typical energy demand of households [6], and variation in production profiles enables a larger share of solar power to be integrated into the energy system [7]. Reducing the mismatch between production and consumption and, thus, balancing the power in the grids is, in fact, one of the rising areas of interest in the field.

Considering the relevance of BPV technologies in commercial applications, accurate estimations of their performance are crucial. The performance [8] and stability [9] of solar panels are strongly affected by the operating temperature, which highlights the necessity of reliable thermal modeling. However, the existing literature reveals a gap in the performance analysis of different thermal models validated with the experimental data collected from PV systems with different installation configurations and technologies [10]. To advance PV thermal modeling, the requirements of new PV technologies and installation solutions should be considered. This is relevant because the panel operating temperature depends not only on environmental conditions [11–13] but also on the characteristics of the system, such as the installation configuration [11,13] and cell technology [14,15]. The environmental conditions that affect the operating temperature include, for instance, the ambient temperature, wind speed and direction, and solar radiation impinging on the panel, that is, plane-of-array (POA) irradiance.

A recent literature review [10] on thermal modeling of mono- and bifacial solar panels emphasized the need for thermal modeling of bifacial panels in different installation configurations and validation of the models. Furthermore, the study [10] identified the role of temperature models as a basis for the simulations performed with the majority of commonly used PV modeling software, including PVsyst, PVGIS, HelioScope, and SAM. The panel operating temperature can be estimated using (semi-)empirical temperature models in which information on heat generation and transfer and system characteristics is included in the model parameters [13,16]. This enables the operating temperature to be directly predicted from easily accessible meteorological data. (Semi-)empirical temperature models are practical to apply in power production modeling due to their simplicity. Even so, many software applications lack a suitable temperature model for BPV panels or the model has constraints [10]. Furthermore, because BPVs have become popular only recently, there is limited amount of long-term data sets available. Long-term temperature data are required to produce panel-specific temperature model parameters, for instance. When the availability of experimental data is limited, the use of temperature data generated through computational simulation offers an alternative for determining model parameters [14]. However, studies evaluating the use of computationally simulated temperature data for determining the model parameters for BPV are missing.

Despite the scarcity of suitable models for BPV panels, only a limited number of studies have suggested modifications to temperature models to account for the irradiance received by the rear surface of the panel [17–22]. Furthermore, of these studies, only a few have experimentally validated the suggested modifications or investigated the suitability of temperature model parameters reported in the literature (i.e., standard parameters) for BPV panels [20–22]. Additionally, the conclusions of their analyses contrast with each other in some respects. For instance, Riley et al. [20] suggested that Sandia model parameters for monofacial photovoltaic (MPV) panels can be reused for BPV panels, while Mannino et al. [21] showed that determining specific parameters for BPV panels improves the accuracy of the temperature estimation notably. Furthermore, de Oliveira et al. [22] presented noticeable differences between the bifacial-specific Faiman parameters and the standard ones. Similarly, the PVsyst model was reported to introduce significant errors in temperature estimation with the standard parameters [22]. These few studies evaluating the applicability of existing temperature models to BPV panels focused on systems with tilted mounting [20–22] or a single-axis tracker [22] and similar studies on vertical mounting are lacking. In addition, the experimental data included in analysis were collected from measurement sites located, for instance, in Italy (37.4° N, 15° E) [21] or Brazil (27.4° S, 48.4° W) [22], and locations with high seasonality such as Nordic conditions are missing.

The present study considers vertical mounting and expands the analysis to Nordic conditions, focusing on low solar elevation angles, as the experimental data were collected from two locations in Southern Finland. In particular, high-latitude locations benefit from VBPV systems during the summer due to the low sun elevation angles and extended daylight hours [7], which underlines the relevance of Nordic countries in bifacial PV research. This study was conducted to 1) validate the applicability of PV temperature models to bifacial panels with different installation configurations; 2) investigate the use of computationally simulated temperature data to predict the missing model parameters for vertically installed bifacial panels and understudied parameters for open-rack mounted ones; and 3) evaluate the need for the bifacial-specific model parameters to help address the discrepancies in the literature. The PV temperature models investigated in the present study were Sandia [13], Faiman [16], and PVsyst [23] models, which are commonly used in commercial PV modeling software [10]. The simulated model parameters were predicted using a physical device thermal model presented in our previous work [14]. The computationally simulated parameters are worth studying due to their independence from experimental data, which enables easy analysis of different PV systems in various geographical locations. Furthermore, experimental data collected from one MPV and two BPV systems, with vertical and open-rack mounting, were used to determine the experimental model parameters and to evaluate the performance of the physical device thermal model and (semi-)empirical models.

2. Experimental data

The experimental panel temperature data were collected from three PV systems: a monofacial system (MPV) [24], a conventionally mounted (open-rack, tilted) bifacial system (CBPV), and a vertically mounted bifacial system (VBPV) [25] (Fig. 1). The MPV system was installed on the rooftop of the Finnish Meteorological Institute's (FMI's) office in Helsinki, Finland [26]. The CBPV and VBPV systems were built at the measurement sites of Turku University of Applied Sciences (TUAS) in Turku, Finland. The specifications of the PV systems are presented in Table 1, and more information on the MPV and VBPV systems can be found in previous contributions [26,27].

In the MPV system, the temperature sensors were placed on the rear surface of the panel close to the point corresponding to the center of the cell. The system has two: one in the southwest (SW) corner and another in the northeast (NE) corner. The temperature data collected from the SW corner were utilized in this study. In the CBPV panel (first panel from the left in Fig. 1(b)), the temperature sensor was installed on the rear surface, while in the VBPV system, they were attached to the front (east-facing) surface of the panels. In addition, the sensors were placed between cells to avoid shading an active area in both bifacial systems. The VBPV system consisted of four panels, and the temperature data used here were collected from one of the panels placed in the middle of the panel array. In this study, the panel temperature refers to the highest (MPV panel) or lowest (CBPV and VBPV panels) temperatures of the panel's rear surface.

Weather and solar radiation data were collected from weather stations near the PV systems. The measurements are listed in Table S2. Of the solar radiation measurements, the POA irradiance received by the front surface of the panel (G_f) and global horizontal irradiance (GHI) measurements were implemented at all weather stations. However, for the CBPV panel, information about POA irradiance received by the rear surface of the panel (G_r) was unavailable. For consistency, G_f and G_r, used as inputs for the temperature models, were calculated based on the observed GHI utilizing the irradiance model.

The data were processed to create appropriate datasets. The studied temperature models are stated to be unsuitable for high resolution input data ($\Delta t \leq 1$ min) [10]. Furthermore, in PV energy production modeling,

Table 1
Photovoltaic system specifications.

	MPV	CBPV	VBPV
PV panel	SolarWorld Protect SW 250 poly	JAM60D10 335/MB/1500V	Prism Solar model Bi60-375BSTC
Tilt angle	15°	45°	90°
Azimuth angle	135°	180°	90°
Latitude	60.20°	60.27°	60.27°
Longitude	24.96°	22.17°	22.17°
Dataset from - to	26/Aug/2015 – 31/Dec/2021	03/Nov/2021 – 31/Mar/2025	18/Aug/2017 – 02/July/2021

(a) (b) (c)

Fig. 1. MPV (a), CBPV (b), VBPV (c) systems located at the measurement sites of FMI at Helsinki (a) and TUAS at Turku (b, c). Original photographs by Karhu/FMI (reproduced from [26] under CC by license) (a) and Anttalainen/University of Turku (b, c).

the use of weather data with a time averaging interval of 15 minutes or less is recommended in the literature [28]. Because the wind speed was measured at a 10-minute interval and it meets the recommendations for both temperature and energy production models, datasets with an averaging interval of 10 minutes were created. In addition, the data point was removed if the value of any relevant model input (GHI, T_{amb}, T_m, or v) was missing.

Data points corresponding to periods during which snow depth on the ground was more than zero were removed from all PV system datasets. Snow cover is a complex factor affecting, for instance, ground albedo, and thus, rear surface gain of the BPV panel. However, its overall impact on PV energy yield is assumed to be small because snow cover mainly occurs during periods with short days and low solar irradiance [29]. Furthermore, PV temperature models are unable to consider the effects of snow when it covers the surface of the PV panel [30], and therefore, snowy periods were excluded from this study. It was expected that snow-free ground implies a snow-free panel surface [30]. The accumulated snow depth data used to filter the MPV system dataset were recorded daily at 00:00 at the weather station close by. Similarly, snow data used to filter the CBPV and VBPV system datasets were collected daily at 06:00 from the Turku Artukainen weather station (60.45° N, 22.18° E).

Irradiance quality control was performed using filtering conditions 1–9 introduced by Gueymard and Ruiz-Arias [31] (see Section S1.4). The night time data points were removed by the filtering condition $\theta_Z \geq 85°$. The filters related to the night time data points and negative GHI, diffuse horizontal irradiance (DHI), and direct normal irradiance (DNI) values rejected most (52%−61%) of the data points. Approximately 0.025%−13% of the remaining points, depending on the PV system, were removed by the other filters.

3. Methods

In this study, physical and semi-empirical thermal models were applied. In the physical thermal model, the modeled MPV and BPV panels were similar in geometry, consisting of front and rear glasses, 72 silicon solar cells (15.6 cm x 15.6 cm), and ethylvinylacetate layers on both sides of the cells. Heat generation in the panels was calculated according to a previously published method [14] including an irradiance and temperature dependent power conversion efficiency (PCE) model [8,32–35] and a band-gap-dependent absorption model [36] (see the applied parameters in Table S1). Conductive heat transfer within the panels and convective and radiative heat exchange with the environment were considered [37,38]. The relevant equations are described in the Supporting Information (Section S1.1) and, with further explanation, in our previous work [14].

The (semi-)empirical models, namely Sandia [13], Faiman [16], and PVsyst [23], were modified for the possible rear side irradiance (G_r) of BPVs:

$$T_m = T_{amb} + (G_f + G_r)\exp(bv + a) \quad (1)$$

$$T_m = T_{amb} + (G_f + G_r)/(U_{L1}v + U_{L0}) \quad (2)$$

$$T_m = T_{amb} + [(G_f\,\alpha_{tot}(1 - PCE_{ref,f}) + G_r\,\alpha_{tot}(1 - PCE_{ref,r}))]/(U_1 v + U_0), \quad (3)$$

where T_m and T_{amb} are the module and ambient temperatures, respectively, b, a, U_{L1}, U_{L0}, U_1, and U_0 are system-specific model parameters, G_f is the front side irradiance, α_{tot} is an absorption parameter (here 0.9 [23]), and $PCE_{ref,f}$ and $PCE_{ref,r}$ are the front and rear side PCEs, respectively. In the case of monofacial panels, $G_r = 0$ and $PCE_{ref,r} = 0$. These models were fitted to the experimental and simulated panel temperature data in the linearized forms with reference to the wind speed (see Section S1.2) to find the model parameters for the different PV systems.

The commercial software PVsyst [39] was applied to model the annual PV energy production using both the predicted panel-specific and the standard temperature model parameters. The annual energy production of the CBPV and VBPV systems in Turku was estimated using synthetic hourly weather data generated in PVsyst. The modeled CBPV and VBPV panels corresponded to those installed at the TUAS' measurement sites (Table 1).

When the total irradiance received by the solar panels was modeled, the plane-of-array irradiance (G_{POA}) was determined utilizing the Purdue Bifacial irradiance model from PVLIB Toolbox [40] presented with more specifics in the Supporting Information (Section S1.3). G_{POA} consists of the beam (G_{beam}), diffuse (G_{diff}), and ground-reflected (G_{refl}) components. G_{beam} was defined as the product of the DNI and the cosine of the angle of incidence [41], while G_{diff} was calculated from the DHI according to the model presented by Perez et al. [42,43]. The Perez1 decomposition model, also referred to as the DIRINT model [44], was applied for the decomposition of the GHI into the DHI and DNI. G_{refl} was calculated using a view-factor based approach described by Sun et al. [18]. Albedo of the PV installation environment was set to 0.18, which describes the reflectivity of an urban environment [30]. In addition, the angular reflection losses of the panels were considered by adapting the

model presented by Martin and Ruiz [45,46]. The angular loss coefficient of 0.16, a typical value for commercial silicon panels [47], was applied.

4. Model validation

4.1. Physical device thermal model validation

A physical device thermal model was used to simulate the operating temperatures of MPV, CBPV, and VBPV panels under varying environmental conditions. The electrical parameters used as an input values corresponded to those reported for the panels from which the experimental temperature data were collected (Table 1). For validation of the thermal model, a set of data points that represent actual PV operating conditions was selected from the dataset (see Section S2.1) and the panel operating temperatures were simulated under these selected conditions.

The accuracy of the present thermal model was evaluated by comparing the simulation results with the experimental validation data (Fig. 2). The operating temperatures were first simulated using a literature value for convective heat transfer coefficient ($h = 3\,(\mathrm{Ws/m^3K})\,v + 2.8\,(\mathrm{W/m^2K})$) and then using an h value optimized for each system. The optimized h values and the description of the optimization procedure can be found in the Supporting Information (Section S2.2). The thermal model allows solving the average, minimum, and maximum temperatures of each component of the panel, such as the cell and rear surface. The simulations performed in our previous work [14] show that the panel temperature reaches its maximum value close to the centers of the cells and decreases toward the inter-cell gaps. Therefore, the measured temperatures were compared to either the simulated maximum or minimum temperature of the rear surface of the panel depending on whether the temperature sensors are located at the point corresponding to the center of the cell (MPV panel) or between cells (CBPV and VBPV panels).

The temperature estimation accuracy of our model increased in all cases when the optimized h value was applied instead of the literature value (Table 2). In particular, the VBPV panel simulations benefited from the optimization of the convective heat transfer coefficient because RMSE decreased from 5.1 °C to 3.1 °C and the bias from −3.9 °C to −0.24 °C (Table 2). Going forward, the optimized convective heat transfer coefficients (Table S3) were utilized.

Table 2
The root-mean-square error (RMSE), mean absolute error (MAE), correlation coefficient (corr. coeff.), and bias of the operating temperatures of MPV, CBPV, and VBPV panels simulated with the physical device thermal model using unoptimized (initial) and optimized convective heat transfer coefficients.

	RMSE [°C]	MAE [°C]	Corr. Coeff.	Bias [°C]
Initial				
MPV	3.1	2.3	0.957	−0.11
CBPV	2.9	2.2	0.968	−0.90
VBPV	5.1	4.4	0.954	−3.9
Optimized				
MPV	2.8	2.2	0.966	−0.051
CBPV	2.8	2.0	0.968	0.16
VBPV	3.1	2.5	0.957	−0.24

4.2. Irradiance model validation

Validation of the irradiance model was carried out by comparing the calculated solar irradiances with the experimental ones (Fig. 3). The experimental irradiance data, which were included in the model validation, were filtered as described in Section 2. The averaging interval of 10 minutes was used in all cases. In the validation of the CBPV irradiance model, only G_f was taken into account because measured G_r was unavailable. When validating the VBPV irradiance model, G_r was also considered. In the literature, PV irradiance models have been observed to perform more reliably for south-facing tilted panels than for vertical panels, due to assumptions related to the modeling of ground-reflected irradiance, for instance [41,48]. Therefore, G_r of the CBPV panel is likely to be estimated more accurately than that of the VBPV panel.

The results indicated that the irradiance received by the MPV and CBPV panels can be estimated with good accuracy using the present irradiance model (Figs. 3(a) and (b)). The MPV and CBPV panels showed RMSEs of around 58 $\mathrm{W/m^2}$ and 53 $\mathrm{W/m^2}$, respectively. Furthermore, the correlation coefficient exceeded 0.98 in both cases (Table 3). In the case of the VBPV panel, there was more variability in the irradiance estimation (Fig. 3(c)). The RMSEs of solar irradiance estimation were 73 $\mathrm{W/m^2}$ and 60 $\mathrm{W/m^2}$ for the front (east-facing) and rear (west-facing) surfaces of the VBPV panel, respectively. The correlation coefficients were approximately 0.96 and 0.97 for the front and rear surfaces (Table 3). The model overestimated the irradiance received by the east-facing surface with a bias of 25 $\mathrm{W/m^2}$. In contrast, irradiance received by the west-facing surface was underestimated with a bias of −17 $\mathrm{W/m^2}$ (Table 3). The results aligned with those previously reported. Manni et al. [49] reported that using the same decomposition and transposition models to predict the solar irradiance received by both the east- and west-facing surfaces results in an overestimation of the irradiance from one surface and its underestimation from the other surface. Manni et al. [49] utilized the data collected from the same VBPV system at the TUAS measurement site in their study, which makes the observations highly comparable.

The difference between the panel and ambient temperatures increases linearly with increasing solar irradiance, by around 0.021°C /($\mathrm{W/m^2}$) (Figure S2). In other words, when the model over- or underestimates the G_{POA} by 100 $\mathrm{W/m^2}$ or less, the impact on the estimated operating temperature is at most 2.1 °C. It is reasonable to assume that the error does not exceed this in any of the cases studied.

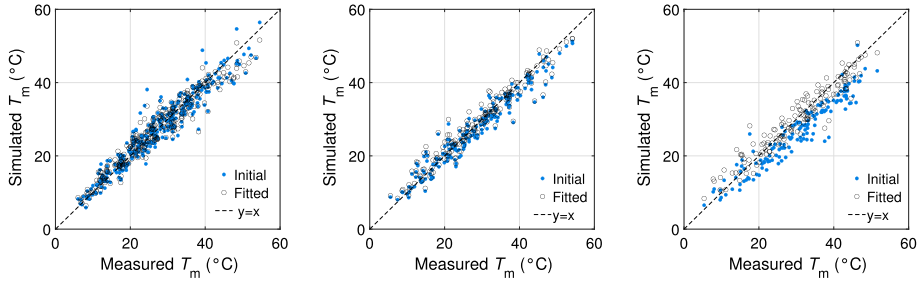

Fig. 2. The operating temperatures simulated using the convective heat transfer coefficient optimized by fitting (black circles) and the unoptimized coefficient from the literature (blue dots) as a function of the temperatures measured from a) MPV, b) CBPV, and c) VBPV panels. (For interpretation of the references to colour in this Figure legend, the reader is referred to the web version of this article).

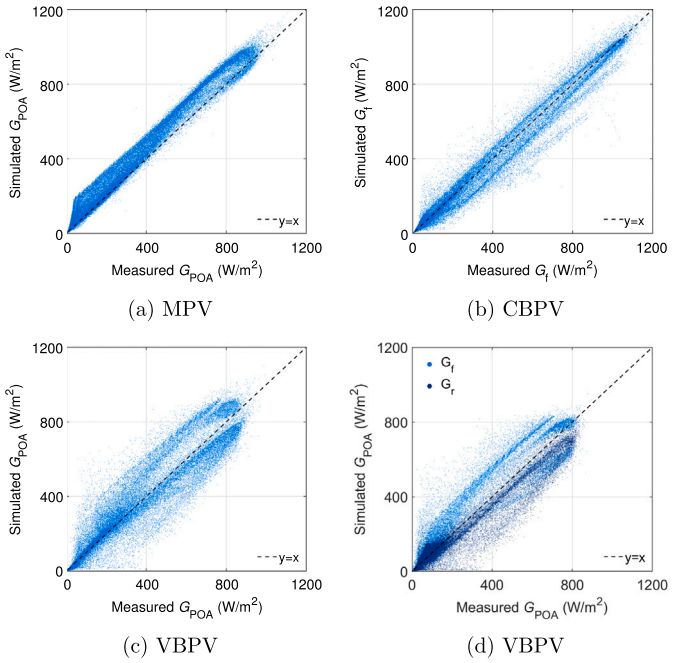

Fig. 3. Estimated G as a function of G measured from MPV (a), CBPV (b), and VBPV (c, d) measurement sites. For the CBPV panel, validation of the irradiance model is limited to the irradiance received by its front surface G_f. For the VBPV panel, the irradiance model is validated with G_{POA} (c) and, in addition, separately with G_f and G_r (d).

Table 3
RMSE, MAE, correlation coefficient, and bias of the estimated irradiance received by the front (G_f) and/or rear (G_r) surfaces of the PV panels.

	RMSE [W/m^2]	MAE [W/m^2]	Corr. Coeff.	Bias [W/m^2]
MPV (G_f)	58	39	0.990	36
CBPV (G_f)	53	34	0.986	−10
VBPV (G_{POA})	94	66	0.939	7.9
VBPV (G_f | G_r)*	73 | 60	43 | 35	0.957 | 0.971	25 | − 17

5. Results

5.1. Applicability of PV temperature models to bifacial panels

In this section, the applicability of PV temperature models to estimate the operating temperatures of bifacial panels with different installation configurations is validated. For this purpose, the linearized Sandia, Faiman, and PVsyst models were first fitted to the experimental data from the CBPV and VBPV panels, as described in Section S1.2 (Fig. 4(d)–(i)). The models were also fitted to the experimental data from the MPV panel for comparison (Fig. 4(a)–(c)). The experimental data applied to the linearized temperature models were filtered as specified in Section 2. In addition, the data points where G_{POA} was below 200 W/m^2 or above 1000 W/m^2 and T_{amb} was below 5 °C or above 30 °C were excluded so that the environmental conditions present in the experimental data were consistent with the simulation conditions.

The linearized temperature models fit all datasets, as Fig. 4 shows. The data points were spread over a wide area, but the number of data points farther from the linear fit was significantly smaller than the number of points close to it (Fig. 4). Despite the large scattering, the most frequently occurring data points showed a stronger linear correlation compared to all observations. The experimental temperature model parameters were obtained from the slope and intercept coefficients of the linear fits (Fig. 4), and they are listed in Table 4.

The experimentally determined model parameters were applied to Sandia, Faiman, and PVsyst models (Eqs. (1)–(3)) to estimate the operating temperatures. The estimated operating temperatures were compared with the measured ones (Figure S3), and the RMSEs of the temperature models for the MPV, CBPV and VBPV panels were determined (Table 5). All the studied temperature models estimated the operating temperatures of the MPV and CBPV panels, with the RMSE being around 2.1 °C – 2.2 °C (Table 5). For the VBPV panel, the RMSE of the estimated operating temperatures was around 2.9 °C – 3.0 °C, which means that the accuracy of the temperature estimation was reduced by 0.7 °C – 0.8 °C compared to the MPV and CBPV panels (Table 5). The bias was small for all the temperature models and panel types studied, with a maximum absolute value of 0.49 °C. A similar estimation accuracy of the MPV and CBPV panel operating temperatures demonstrates that common PV temperature models are applicable to bifacial panels when they are modified to account for the rear surface irradiance.

5.2. Computationally simulated model parameters for bifacial panels

With the computationally simulated temperature model parameters, the thermal behavior of several types of PV systems can be studied without the need for experimental data. For instance, the electrical properties as well as geographical location and installation configuration of a PV system can be easily modified. In this section, it is investigated whether computationally simulated temperature data can be reliably used to predict PV temperature model parameters and panel operating temperatures.

The simulated model parameters were predicted by fitting linearized temperature models to the temperature data obtained from the physical device thermal model (Figure S4). To generate the temperature data, the panel operating temperatures were modeled under varying ambient conditions, specifically wind speeds of 0 – 10 m/s, ambient temperatures of 5 – 30 °C, and plane-of-array irradiances of 200 – 1000 W/m^2. The G_{POA} values were calculated from measured GHI using the irradiance model (Section S1.3). The temperature model parameters predicted using these simulated temperature data are presented in Table 4.

Furthermore, the operating temperatures were estimated by applying the simulated parameters to the temperature models (Figure S5). Using Sandia, Faiman, and PVsyst models, the RMSEs for the MPV, CBPV, and VBPV panels were 2.1 °C, 2.2 °C and 2.9 °C, respectively (Table 5). The RMSE values obtained with the experimental and simulated model parameters differed from each other by around 0.1 °C at most. In addition, bias was within the same order of magnitude in all the cases. A good agreement between the operating temperatures estimated using the experimental and simulated parameters validates the use of computationally simulated temperature data in predicting model parameters and panel temperature. Furthermore, this finding highlights the potential of computational methods in analyzing the thermal behavior of new PV technologies without the need for long-term field measurements.

The performance of the experimental and simulated temperature model parameters was also evaluated on a daily level. Two consecutive days were selected from the measurement period of the CBPV and VBPV systems, one of which represented a sunny day and the other a day with more fluctuating cloud cover (Fig. 5). The estimated operating temperatures aligned well with the measured ones, especially on sunny day. The difference between the estimated and measured temperatures was more noticeable on a cloudy day.

The studied (semi-)empirical temperature models are steady-state models, meaning that they predict the temperature at a particular time and omit the evolution of temperature over time. Therefore, these models have constraints when environmental conditions, such as irradiance, change rapidly. Indeed, on cloudy days the modeled temperature peaks are higher and valleys lower in temperature while in reality, it takes some time for the panel to heat up and cool down, resulting in somewhat less variation in temperature (Fig. 5). For this reason, steady-state temperature models also introduce errors to the power output estimations.

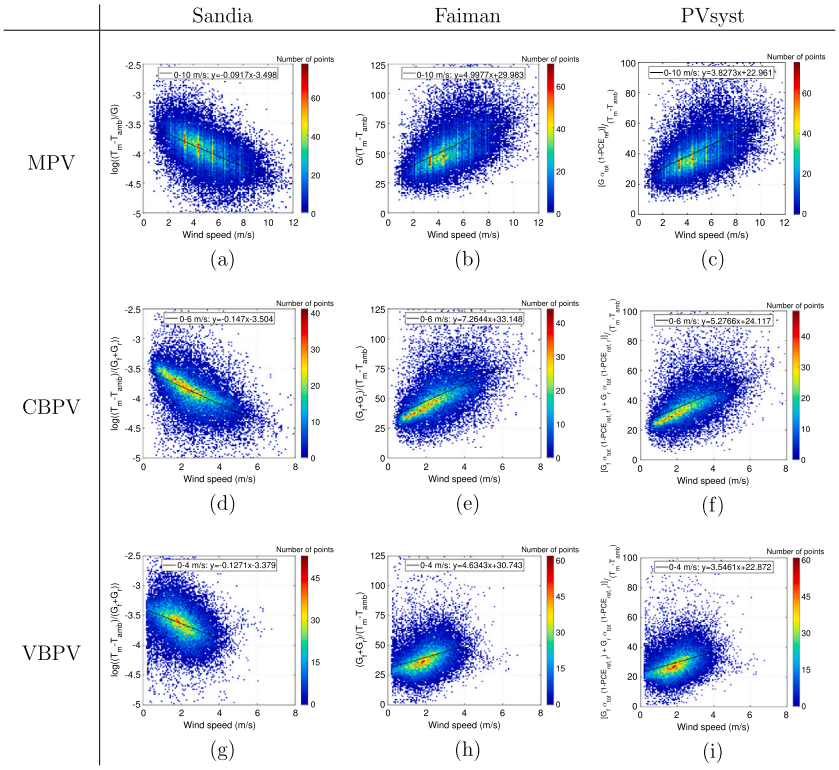

Fig. 4. Linearized Sandia (a, d, g), Faiman (b, e, h), and PVsyst (c, f, i) models fitted into experimental data from MPV (a–c), CPBV (d–f), and VBPV (g–i) system measurement sites.

However, an error of less than 5 °C in the temperature estimation translates into an impact of less than 3% on the power output, which can be suitable for many engineering purposes [13]. Additionally, the (semi-)empirical temperature models are unable to account for the effects of wind direction, which creates an additional source of error in the temperature estimation, whose significance is discussed in the Supporting Information (Section S3). One of the main conclusions from that discussion is that more extensive experimental data would be needed to make corrections to temperature models to account for the effects of wind direction. This is because the data collected from a single measurement site may reflect the characteristics of that specific site rather than the effects of wind direction in general. Nevertheless, a good overall accuracy combined with the computational simplicity supports the use of these (semi-)empirical temperature models. However, if more accurate estimations are desired, modeling approaches based on machine learning and artificial intelligence, for instance, have shown a good potential [50].

Furthermore, the experimental and simulated model parameters produced similar estimated operating temperatures throughout the observed period for the CBPV and VBPV panels (Fig. 5). This was expected because the simulated temperature data was shown to perform as accurately in predicting operating temperatures as the experimental data (Table 5).

5.3. Comparison of mono- and bifacial-specific model parameters

In this section, the need for bifacial-specific model parameters is evaluated. First, the simulated model parameters of mono- and bifacial panels with similar electrical and thermal characteristics are compared. Furthermore, it is investigated whether standard parameters, originally determined for monofacial panels, can be reused for bifacial panels and how their temperature estimation accuracy compares with that of the bifacial-specific ones.

Table 4
The Sandia, Faiman, and PVsyst model parameters of MPV, CBPV, and VBPV panels predicted using experimental and computationally simulated data.

	Sandia		Faiman		PVsyst	
	a	b	U_{L0} [W/m^{2}K]	U_{L1} [Ws/m^{3}K]	U_0 [Ws/m^{2}K]	U_1 [Ws/m^{3}K]
Experimental						
MPV	−3.50	−0.0917	30.0	5.00	23.0	3.83
CBPV	−3.50	−0.147	33.1	7.26	24.1	5.28
VBPV	−3.38	−0.127	30.7	4.63	22.9	3.55
Simulated						
MPV	−3.60	−0.0715	34.0	3.80	26.0	2.91
CBPV	−3.46	−0.149	27.7	7.70	20.1	5.61
VBPV	−3.46	−0.102	31.0	4.15	23.1	3.14

The results show that the predicted temperature model parameters of different PV panels varied (Table 4). However, the observed panels also differed from each other in terms of the tilt and azimuth angles as well as the electrical and thermal parameters (Table 1). Therefore, it is unjustified to directly compare the predicted model parameters of these panels. The suitability of MPV model parameters to estimate the operating temperatures of BPV panels, with a consistent installation configuration, was evaluated by simulating the operating temperatures of the MPV and CBPV panels under the same convective cooling conditions and with similar electrical and thermal parameters. In other words, the only difference between the MPV and CBPV panel simulations was that the rear surface irradiance was excluded from the MPV panel simulation. Additionally, the operating temperatures of the VBPV panel were simulated using the electrical and thermal parameters of the CBPV panel while maintaining the cooling conditions of the VBPV panel. These simulated operating temperatures were used to predict

Table 5
RMSEs and biases of the operating temperatures of MPV, CBPV, and VBPV panels estimated with the Sandia, Faiman and PVsyst models using experimental and simulated model parameters.

	Sandia		Faiman		PVsyst	
	RMSE [°C]	Bias [°C]	RMSE [°C]	Bias [°C]	RMSE [°C]	Bias [°C]
Experimental						
MPV	2.12	0.35	2.16	0.15	2.16	0.15
CBPV	2.15	0.18	2.21	−0.20	2.22	−0.20
VBPV	2.95	0.0055	2.90	−0.46	2.90	−0.49
Simulated						
MPV	2.13	0.32	2.13	0.30	2.13	0.30
CBPV	2.18	0.42	2.18	0.42	2.18	0.43
VBPV	2.90	−0.33	2.90	−0.34	2.91	−0.34

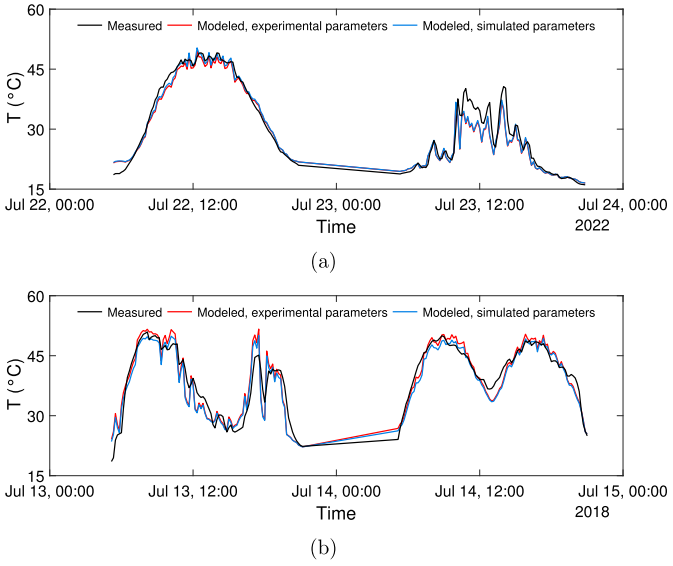

Fig. 5. The operating temperatures of (a) CBPV and (b) VBPV panels estimated with a Sandia model using experimental (red line) and simulated (blue line) model parameters. The measured operating temperature (black line) is provided for comparison. (For interpretation of the references to colour in this Figure legend, the reader is referred to the web version of this article).

Table 6
The temperature model parameters predicted for the MPV, CBPV, and VBPV panels using the temperature data simulated with the electrical parameters of the CBPV panel.

	Sandia		Faiman		PVsyst	
	a	b	U_{L0} [W/m^{2}K]	U_{L1} [Ws/m^{3}K]	U_0 [W/m^{2}K]	U_1 [Ws/m^{3}K]
MPV	−3.46	−0.149	27.8	7.75	20.1	5.63
CBPV	−3.46	−0.149	27.7	7.70	20.1	5.61
VBPV	−3.50	−0.102	31.5	4.73	22.9	3.44

* Tilt angles (and, thus, convective cooling conditions) of the panels simulated with MPV and CBPV models are equal ($\theta_T = 45°$).

comparable model parameters for the MPV, CBPV, and VBPV panels (Table 6).

The model parameters of the MPV and CBPV panels, predicted using the temperature data simulated under the same environmental conditions and electrical parameters, were very similar (Table 6). The model parameters of the VBPV panel differed from those of the MPV and CBPV panels more in terms of the wind-dependent model parameters (b, U_{L1}, U_1), which was expected due to the different tilt angles and, thus, convective cooling of the panels (Table 6). When MPV-specific model parameters were applied to the CBPV panel instead of CBPV-specific ones, the impact on the accuracy of CBPV panel operating temperature estimation was negligible. Similarly, applying MPV-specific model parameters to the VBPV panel resulted in a decrease of around 0.1 °C in RMSE across all the studied temperature models. Thus, it is reasonable to expect that when mono- and bifacial panels share similar electrical characteristics, the operating temperatures can be estimated using the same parameters, given that the irradiance is appropriately modeled.

A sensitivity analysis was performed on CBPV and VBPV panels to further investigate the effects of the electrical parameters on the operating temperatures and model parameters of PV panels. $PCE_{ref,f}$ of the CBPV and VBPV panels was varied between 14% and 22% and the temperature coefficient of efficiency (β_T) between −0.45 %/°C and −0.25 %/°C. The efficiency of the rear surface was expected to be 70% of that of the front surface. Additionally, the effects of below-band gap absorption ($\alpha_{\lambda \geq \lambda_g}$) were studied by varying it between 0% and 50%. The data points included in the sensitivity analysis represented the following conditions: ambient temperatures from 10 °C to 30 °C with steps of 10 °C, wind speeds from 1 m/s to 6 m/s with steps of 1 m/s (0.5 m/s for VBPV panel), and irradiances from 300 W/m^2 to 900 W/m^2 with steps of 300 W/m^2.

The sensitivity analysis demonstrated significant variations in the temperature model parameters, especially as a function of $PCE_{ref,f}$ and $\alpha_{\lambda \geq \lambda_g}$ (Figures S6–S9). These variations led to notable differences in the estimated PV operating temperatures (Figure S10). For instance, under normal operating conditions (T_{amb} = 20 °C, v = 1 m/s, G_{POA} = 800 W/m^2), the estimated operating temperature of the CBPV panel decreased by 2.4 °C, across all studied models, when $PCE_{ref,f}$ used for predicting the model parameters increased from 14% to 22% (Figure S10a). The corresponding change in the operating temperature of the VBPV panel was 2.1 – 2.4 °C, depending on the temperature model (Figure S10c). Furthermore, the estimated operating temperatures of both panels increased by 3.2 – 3.3 °C when $\alpha_{\lambda \geq \lambda_g}$ used to predict the model parameters increased from 0% to 50% (Figures S10b and S10d). Variations in β_T did not have a significant effect on the panel operating temperatures (Figures S10a and S10c).

The challenge with the temperature model parameters presented in the literature (i.e., standard parameters) is that they are likely to best describe the operating temperatures of PV systems that are similar to the systems based on which the model parameters were originally determined. For example, the standard parameters of the Sandia model for open-rack mounted panels (a = −3.47, b = −0.0594) were introduced in 2004 [13], since then the electrical efficiency of PV panels has significantly increased. Similarly, the standard parameters of the Faiman model (U_{L0} = 25 W/m^{2}K, U_{L1} = 6.84 Ws/m^{3}K) were experimentally determined for panels with a glass-cell-backsheet (Tedlar) structure in 2008 [16]. The standard parameters suggested by PVsyst (U_0 = 25 W/m^{2}K, U_1 = 1.2 Ws/m^{3}K) were defined based on experimental data from several panels with different installations (open-rack, facade) and cell types (mono- and polycrystalline silicon) [23]. The operating temperatures of the CBPV and VBPV panels were estimated using the standard parameters to evaluate their applicability to bifacial panels. The RMSEs of these estimates were compared against RMSEs obtained using the simulated and experimental parameters (Fig. 6). The simulated parameters were predicted under varying $PCE_{ref,f}$ values.

The use of standard parameters resulted in a significantly lower estimation accuracy of CBPV panel operating temperatures than the use of simulated or experimental parameters for all studied temperature models (Fig. 6(a)–(c)). The RMSE for the CBPV panel was reduced by at least 0.2 – 1.2 °C, depending on the temperature model, when the simulated parameters were applied instead of the standard ones. The simulated model parameters outperformed the standard ones, even when the PCE

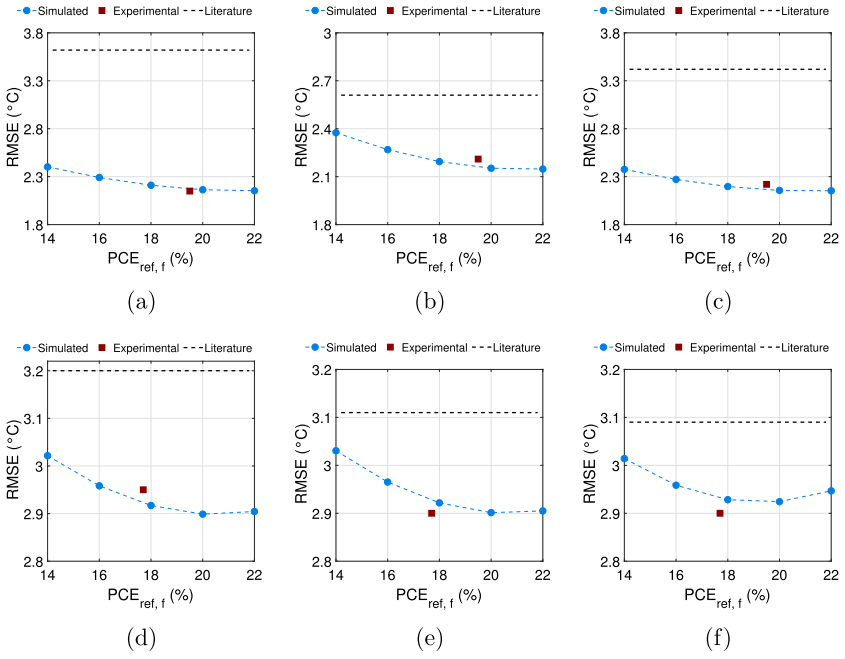

Fig. 6. RMSEs of the CBPV (a–c) and VBPV (d–f) panel operating temperatures estimated with Sandia (a, d), Faiman (b, e) and PVsyst (c, f) models using the simulated (blue line), experimental (red square), and standard parameters (black dashed line). The simulated model parameters were predicted under varying $PCE_{ref,f}$. The PCEs of the PV systems based on which the standard parameters were determined are unavailable. (For interpretation of the references to colour in this Figure legend, the reader is referred to the web version of this article).

used for predicting the simulated model parameters did not correspond well to the actual PCE reported for the studied panel. In contrast, the RMSEs of the estimated operating temperatures of VBPV panel were relatively similar regardless of whether the simulated, experimental, or standard parameters were utilized (Fig. 6(d)–(f)). However, the simulated model parameters still outperformed the standard ones under all studied $PCE_{ref,f}$ values. The results indicate that the standard parameters were more suitable for estimating the operating temperatures of a PV system with a lower PCE and a higher β_T (here a VBPV panel) than vice versa (here a CBPV panel).

Overall, the temperature model parameters presented in the literature can, at worst, lead to notable inaccuracies in temperature estimations, but at best, provide reasonable estimation accuracy. Furthermore, the annual energy production of the CBPV and VBPV panels was estimated with PV modeling software (PVsyst) using both the simulated panel-specific parameters (Table 4) and the standard parameters of the PVsyst temperature model. The resulting difference in the estimated annual production was around 0.3% for the CBPV panel and around 0.2% for the VBPV panel. The difference is relatively small; however, for a large utility-scale PV plant, such a difference can result in significant variations in the estimated annual revenue [51,52]. Therefore, the use of standard parameters in temperature estimations should be assessed depending on the accuracy required for a specific case.

6. Conclusions

In this study, the applicability and accuracy of Sandia, Faiman, and PVsyst temperature models for different bifacial panels were investigated. Furthermore, bifacial-specific temperature model parameters were extracted from experimental data. The parameters were also predicted using computationally simulated data and then compared to the experimental ones to demonstrate the possibility of producing reliable temperature estimations computationally. Finally, the suitability of monofacial-specific parameters for estimating the operating temperatures of bifacial panels was evaluated to help address the discrepancies in the literature.

The results revealed that the studied PV temperature models are applicable to bifacial panels with different installation configurations. The linearized temperature models demonstrated reasonable alignment with the most frequently occurring experimental data points collected from the vertical and open-rack mounted systems. Furthermore, the close match between simulated and experimental model parameters confirmed that computationally simulated temperature data can be used to predict model parameters reliably. Finally, it was observed that the use of literature parameters can lead to significant inaccuracies in the temperature estimations of bifacial panels; however, if the mono- and bifacial panels are relatively similar in their electrical, optical, and thermal characteristics, the same temperature model parameters can be applied.

This study responded to the identified need for validation of bifacial PV thermal models. Based on the results, it is recommended to consider the effects of the installation configuration and the electrical characteristics of the panel on the bifacial-specific temperature model parameters for accurate operating temperature estimation. In general, the findings improve prediction of the temperature-dependent output power of BPV in different installations. Additionally, predicting model parameters through simulation, which was found to be a reliable approach, provides an opportunity to determine model parameters for new photovoltaic technologies and panel types, even when long-term measurement data are not available.

CRediT authorship contribution statement

Julianna Varjopuro: Writing – original draft, Visualization, Formal analysis, Conceptualization. **Aleksi Kamppinen:** Writing – review & editing, Supervision. **Aapo Poskela:** Writing – review & editing. **Anders V. Lindfors:** Writing – review & editing, Resources. **Shuo Wang:** Writing – review & editing, Investigation. **Samuli Ranta:** Resources.

Kati Miettunen: Writing – review & editing, Supervision, Funding acquisition.

Declaration of competing interest

The authors declare the following financial interests/personal relationships which may be considered as potential competing interests:

Co-author served as an Associate Editor for Solar Energy during 2020–2023 (A. V. Lindfors). Given his previous role as Associate Editor of Solar Energy, he had no involvement in the peer review of this article and had no access to information regarding its peer review. Full responsibility for the editorial process for this article was delegated to another journal editor. If there are other authors, they declare that they have no known competing financial interests or personal relationships that could have appeared to influence the work reported in this paper.

Acknowledgements

J.V., S.W., A.V.L., S.R. and K.M. acknowledge RealSolar project (358542, 358543, 358541), which is funded by the Strategic Research Council (SRC) established within the Research Council of Finland. A.K. thanks University of Turku Graduate School (UTUGS) and Lieto Savings Bank Foundation (KesPV project). We thank Magda Szarek from the University of Turku for PVsyst annual energy production simulations.

Appendix A. Supplementary data

Supplementary data for this article can be found online at doi:10.1016/j.solener.2026.114529.

Data availability

Datasets supporting this study can be found at data repositories hosted by Finnish Meteorological Institute (DOI: 10.57707/fmi-b2share.tn0wb-as670, MPV data) and Turku University of Applied Science (https://nerc.turkuamk.fi/data-portal/, VBPV data). Simulation scripts are openly available on Github (https://github.com/juliavarjop/temperature_modeling_parameters_for_bpv.git).

References

[1] International Renewable Energy Agency (IRENA), Future of Solar Photovoltaic: Deployment, Investment, Technology, Grid Integration and Socio-Economic Aspects, 2019.
[2] International Energy Agency (PVPS), Snapshot of Global Markets, 2024, https://doi.org/10.69766/VHRF4040
[3] D. Heenatigala Kankanamge, J. Jääskeläinen, S. Jouttijärvi, S. Syri, Economic viability of large-scale solar PV implementation in the nordic power market: case Finland, Renew. Energy Focus 56 (2026) 100750, https://doi.org/10.1016/j.ref.2025.100750
[4] A. Carrod, A. Ghosh, A review of bifacial solar photovoltaic applications, Front. Energy 17 (2023) 704–726, https://doi.org/10.1007/s11708-023-0903-7
[5] S. Jouttijärvi, G. Lobaccaro, A. Kamppinen, K. Miettunen, Benefits of bifacial solar cells combined with low voltage power grids at high latitudes, Renew. Sustain. Energy Rev. 161 (2022) 112354, https://doi.org/10.1016/j.rser.2022.112354
[6] S. Jouttijärvi, L. Karttunen, S. Ranta, K. Miettunen, Techno-economic analysis on optimizing the value of photovoltaic electricity in a high-latitude location, Appl. Energy. 361 (2024) 122924, https://doi.org/10.1016/j.apenergy.2024.122924
[7] S. Jouttijärvi, J. Thorning, M. Manni, H. Huerta, S. Ranta, M. Di Sabatino, G. Lobaccaro, K. Miettunen, A comprehensive methodological workflow to maximize solar energy in low-voltage grids: a case study of vertical bifacial panels in nordic conditions, Solar Energy 262 (2023) 111819, https://doi.org/10.1016/j.solener.2023.111819
[8] M.A. Green, General temperature dependence of solar cell performance and implications for device modelling, Prog. Photovolt. Res. Appl. 11 (5) (2003) 333–340, https://doi.org/10.1002/pip.496
[9] A. Ndiaye, A. Charki, A. Kobi, C.M.F. Kébé, P.A. Ndiaye, V. Sambou, Degradations of silicon photovoltaic modules: a literature review, Sol. Energy 96 (2013) 140–151, https://doi.org/10.1016/j.solener.2013.07.005
[10] A. Osama, G.M. Tina, A. Gagliano, Thermal models for mono/bifacial modules in ground/floating photovoltaic systems: a review, Renew. Sustain. Energy Rev. 216 (2025) 115627, https://doi.org/10.1016/j.rser.2025.115627
[11] S. Armstrong, W.G. Hurley, A thermal model for photovoltaic panels under varying atmospheric conditions, Appl. Therm. Eng. 30 (11) (2010) 1488–1495, https://doi.org/10.1016/j.applthermaleng.2010.03.012
[12] M. Akhsassi, A. El Fathi, N. Erraissi, N. Aarich, A. Bennouna, M. Raoufi, A. Outzourhit, Experimental investigation and modeling of the thermal behavior of a solar PV module, Sol. Energy Mater. Sol. Cells 180 (2018) 271–279, https://doi.org/10.1016/j.solmat.2017.06.052
[13] D.L. King, W.E. Boyson, J.A. Kratochvil, Photovoltaic Array Performance Model, Tech. rep., Sandia National Laboratories, 2004, https://doi.org/10.2172/919131
[14] J. Varjopuro, A. Kamppinen, A. Poskela, J.A. Karhu, A.V. Lindfors, K. Miettunen, Computational simulation of perovskite and silicon solar panel operating temperatures in varying ambient conditions, Sol. Energy Mater. Sol. Cells 290 (2025) 113657, https://doi.org/10.1016/j.solmat.2025.113657
[15] M. Koehl, M. Heck, S. Wiesmeier, J. Wirth, Modeling of the nominal operating cell temperature based on outdoor weathering, Sol. Energy Mater. Sol. Cells 95 (7) (2011) 1638–1646, https://doi.org/10.1016/j.solmat.2011.01.020
[16] D. Faiman, Assessing the outdoor operating temperature of photovoltaic modules, Prog. Photovolt. Res. Appl. 16 (4) (2008) 307–315, https://doi.org/10.1002/pip.813
[17] G.J.M. Janssen, B.B. Van Aken, A.J. Carr, A.A. Mewe, Outdoor performance of bifacial modules by measurements and modelling, Energy Procedia 77 (2015) 364–373, 5th International Conference on Silicon Photovoltaics, SiliconPV 2015. https://doi.org/10.1016/j.egypro.2015.07.051
[18] X. Sun, M.R. Khan, C. Deline, M.A. Alam, Optimization and performance of bifacial solar modules: a global perspective, Appl. Energy. 212 (2018) 1601–1610, https://doi.org/10.1016/j.apenergy.2017.12.041
[19] M.T. Patel, R.A. Vijayan, R. Asadpour, M. Varadharajaperumal, M.R. Khan, M.A. Alam, Temperature-dependent energy gain of bifacial PV farms: a global perspective, Appl. Energy. 276 (2020) 115405, https://doi.org/10.1016/j.apenergy.2020.115405
[20] D. Riley, C. Hansen, J. Stein, M. Lave, J. Kallickal, B. Marion, F. Toor, A performance model for bifacial PV modules, in: 2017 IEEE 44th Photovoltaic Specialist Conference (PVSC), 2017, pp. 3348–3353, https://doi.org/10.1109/PVSC.2017.8366045
[21] G. Mannino, G.M. Tina, M. Cacciato, L. Todaro, F. Bizzarri, A. Canino, Experimental assessment of temperature estimation models of bifacial photovoltaic modules, in: 2022 IEEE 49th Photovoltaics Specialists Conference (PVSC), 2022, pp. 0214–0216, https://doi.org/10.1109/PVSC48317.2022.9938792
[22] A. Kirsten Vidal de Oliveira, M. Braga, H.F. Naspolini, R. Rüther, Validation of thermal models for bifacial photovoltaic systems under various albedo conditions, Prog. Photovolt. Res. Appl. (2025), https://doi.org/10.1002/pip.3892
[23] PVsyst, Array thermal losses, https://www.pvsyst.com/help/project-design/array-and-system-losses/array-thermal-losses/ (accessed 26 August 2025).
[24] J.A. Karhu, A.V. Lindfors, PV Production Data with Ancillary PV and Meteorological Data Including Solar Radiation Measurements from FMI's Outdoor Solar Laboratories in Helsinki, Kuopio and Sodankylä (Finland) Starting from August 2015 and Ending Dec 2021 [Data Set], 2025, https://doi.org/10.57707/fmi-b2share.tn0wb-as670
[25] NERC, Data portal – new energy research center turku, https://nerc.turkuamk.fi/data-portal/ (accessed 14 November 2025).
[26] J.A. Karhu, A.V. Lindfors, W. Wandji Nyamsi, T. Salola, A. Poikonen, M.R.A. Pitkänen, T. Mielonen, O. Mantikka, Photovoltaic power and meteorological datasets with snow detection from the outdoor solar power laboratories of the Finnish meteorological institute, Geosci. Data J. 13 (1) (2026) e70039, https://doi.org/10.1002/gdj3.70039
[27] L. Karttunen, S. Jouttijärvi, A. Poskela, H. Palonen, H. Huerta, M. Todorović, S. Ranta, K. Miettunen, Comparing methods for the long-term performance assessment of bifacial photovoltaic modules in nordic conditions, Renewable Energy 219 (2023) 119473, https://doi.org/10.1016/j.renene.2023.119473
[28] C. Hansen, J. Stein, D. Riley, Effect of Time Scale on Analysis of PV System Performance, Tech. rep., Sandia National Laboratories, 2012, https://doi.org/10.13140/2.1.1150.3368
[29] M. Szarek, S. Jouttijärvi, L. Karttunen, T. Hynnä, S. Ranta, K. Miettunen, Performance evaluation of high latitude agrivoltaic systems with vertically mounted bifacial panels, Appl. Energy. 402 (2026) 127022, https://doi.org/10.1016/j.apenergy.2025.127022
[30] H. Böök, A. Poikonen, A. Aarva, T. Mielonen, M.R.A. Pitkänen, A.V. Lindfors, Photovoltaic system modeling: a validation study at high latitudes with implementation of a novel DNI quality control method, Solar Energy 204 (2020) 316–329, https://doi.org/10.1016/j.solener.2020.04.068
[31] C.A. Gueymard, J.A. Ruiz-Arias, Extensive worldwide validation and climate sensitivity analysis of direct irradiance predictions from 1-min global irradiance, Solar Energy 128 (2016) 1–30, special issue: Progress in Solar Energy. https://doi.org/10.1016/j.solener.2015.10.010
[32] M.A. Green, Solar Cells: Operating Principles, Technology, and System Applications, Prentice-Hall, Englewood Cliffs, NJ, USA, 1982.
[33] W. Shockley, H.J. Queisser, Detailed balance limit of efficiency of p-n junction solar cells, J. Appl. Phys. 32 (3) (1961) 510–519.
[34] K. Emery, J. Burdick, Y. Caiyem, D. Dunlavy, H. Field, B. Kroposki, T. Moriarty, L. Ottoson, S. Rummel, T. Strand, M. Wanlass, Temperature dependence of photovoltaic cells, modules and systems, in: Conference Record of the Twenty Fifth IEEE Photovoltaic Specialists Conference-1996, IEEE, 1996, pp. 1275–1278.
[35] N.H. Reich, W.G.J.H.M. van Sark, E.A. Alsema, R.W. Lof, R.E.I. Schropp, W.C. Sinke, W.C. Turkenburg, Crystalline silicon cell performance at low light intensities, Sol. Energy Mater. Sol. Cells 93 (9) (2009) 1471–1481, https://doi.org/10.1016/j.solmat.2009.03.018
[36] R. Santbergen, J.M. Goud, M. Zeman, J.A.M. van Roosmalen, R.J.C. van Zolingen, The am1.5 absorption factor of thin-film solar cells, Sol. Energy Mater. Sol. Cells 94 (5) (2010) 715–723, https://doi.org/10.1016/j.solmat.2009.12.010
[37] A.D. Jones, C.P. Underwood, A thermal model for photovoltaic systems, Solar Energy 70 (4) (2001) 349–359, https://doi.org/10.1016/S0038-092X(00)00149-3

[38] W. Hu, X. Li, J. Wang, Z. Tian, B. Zhou, J. Wu, R. Li, W. Li, N. Ma, J. Kang, Y. Wang, J. Tian, J. Dai, Experimental research on the convective heat transfer coefficient of photovoltaic panel, Renew. Energy 185 (2022) 820–826, https://doi.org/10.1016/j.renene.2021.12.090
[39] PVsyst, Photovoltaic software, https://www.pvsyst.com/ (accessed 2 March 2026).
[40] Sandia National Laboratories, PVLIB toolbox, https://pvpmc.sandia.gov/tools/pv_lib-toolbox/ (accessed 26 August 2025).
[41] B. Sun, L. Lu, Y. Yuan, P. Ocłoń, Development and validation of a concise and anisotropic irradiance model for bifacial photovoltaic modules, Renew. Energy 209 (2023) 442–452, https://doi.org/10.1016/j.renene.2023.04.012
[42] R. Perez, R. Seals, P. Ineichen, R. Stewart, D. Menicucci, A new simplified version of the perez diffuse irradiance model for tilted surfaces, Solar Energy 39 (3) (1987) 221–231, https://doi.org/10.1016/S0038-092X(87)80031-2
[43] R. Perez, P. Ineichen, R. Seals, J. Michalsky, R. Stewart, Modeling daylight availability and irradiance components from direct and global irradiance, Solar Energy 44 (5) (1990) 271–289, https://doi.org/10.1016/0038-092X(90)90055-H
[44] R. Perez, P. Ineichen, E.L. Maxwell, R.D. Seals, A. Zelenka, Dynamic global-to-direct irradiance conversion models, ASHRAE Trans. 98 (1992) 354–369.
[45] N. Martin, J.M. Ruiz, Calculation of the PV modules angular losses under field conditions by means of an analytical model, Sol. Energy Mater. Sol. Cells 70 (1) (2001) 25–38, https://doi.org/10.1016/S0927-0248(00)00408-6
[46] N. Martin, J.M. Ruiz, Annual angular reflection losses in PV modules, Prog. Photovolt. Res. Appl. 13 (2004) 75–84, https://doi.org/10.1002/pip.585
[47] M.R. Khan, A. Hanna, X. Sun, M.A. Alam, Vertical bifacial solar farms: physics, design, and global optimization, Appl. Energy 206 (2017) 240–248, https://doi.org/10.1016/j.apenergy.2017.08.042
[48] E. Tonita, S. Ovaitt, H. Toal, K. Hinzer, C. Pike, C. Deline, Vertical bifacial photovoltaic system model validation: study with field data, various orientations, and latitudes, IEEE J. Photovoltaics 15 (4) (2025) 600–609, https://doi.org/10.1109/JPHOTOV.2025.3561395
[49] M. Manni, S. Jouttijärvi, S. Ranta, K. Miettunen, G. Lobaccaro, Validation of model chains for global tilted irradiance on East-West vertical bifacial photovoltaics at high latitudes, Renew. Energy 220 (2024) 119722, https://doi.org/10.1016/j.renene.2023.119722
[50] A. Keddouda, R. Ihaddadene, A. Boukhari, A. Atia, M. Arıcı, N. Lebbihiat, N. Ihaddadene, Photovoltaic module temperature prediction using various machine learning algorithms: performance evaluation, Appl. Energy. 363 (2024) 123064, https://doi.org/10.1016/j.apenergy.2024.123064
[51] G.S. Kinsey, Spectrum sensitivity, energy yield, and revenue prediction of PV modules, IEEE J. Photovolt. 5 (1) (2015) 258–262, https://doi.org/10.1109/JPHOTOV.2014.2370256
[52] M. Schweiger, W. Herrmann, C. Monokroussos, U. Rau, Understanding the energy yield of PV modules, Design and Build (Technical Briefing), www.pv-tech.org, May 2017), pp. 56–65.